

## Bandwidth dependence of insulator-metal transitions in perovskite cobalt oxides

S. Yamaguchi, Y. Okimoto, and Y. Tokura

*Department of Applied Physics, University of Tokyo, Tokyo 113, Japan*

(Received 16 July 1996)

Insulator-metal transitions and related electronic structures have been investigated for single crystals of perovskite-type cobalt oxides  $R\text{CoO}_3$  ( $R=\text{La, Pr, Nd, Sm, Eu, and Gd}$ ) with  $R$ -dependent variation of one-electron bandwidth ( $W$ ). All the compounds exhibit the insulating ground state but undergo gradual insulator-metal ( $I$ - $M$ ) transitions at 500–700 K. Systematic variation of the  $I$ - $M$  transition temperatures ( $T_{\text{IM}}$ ) as well as the thermal and optical charge gaps in the insulating phase have been observed with change of  $R$  species (or equivalently  $W$ ). Anomalously low  $T_{\text{IM}}$  as compared with the charge gap in each  $R\text{CoO}_3$  suggests that the  $I$ - $M$  transition should be viewed as a thermally induced Mott transition.

[S0163-1829(96)52640-8]

The perovskite-type oxides  $R\text{MO}_3$ ,  $R$  and  $M$  being a trivalent rare earth ion and  $3d$  transition metal, respectively, are mostly insulating apart from a few compounds of  $M=\text{Ni}$  and  $\text{Cu}$  (e.g.  $\text{LaNiO}_3$  and  $\text{LaCuO}_3$ ).<sup>1-3</sup> In these compounds, the origin of the charge gap can be ascribed to the strong electron correlation of the  $3d$  transition metal  $M^2$  and hence a variety of insulator-metal phenomena show up on the verge of the Mott transition. For example, a series of  $\text{RNiO}_3$  exhibits an electronic phase diagram composed of paramagnetic insulator, antiferromagnetic insulator, and paramagnetic metal phases as a function of the ionic radius of the  $R$ -site,<sup>4</sup> which mimics the electronic phase diagram in the correlated electron system as a function of correlation strength. This is because the substitution of the  $R$ -site modifies the distortion of the perovskite lattice, in particular the  $M$ - $O$ - $M$  bond angle, and hence results in a systematic change of the transfer interaction ( $t_{pd}$ ) between the  $M$   $3d$  and  $O$   $2p$  orbital ( $p$ - $d$  mixing). In this paper, we report on the systematic change of the insulator-metal (IM) phenomena with such an  $R$ -site variation for the case of  $R\text{CoO}_3$  ( $R=\text{La, Pr, Nd, Sm, Eu, and Gd}$ ).

Among the  $R\text{MO}_3$  perovskites,  $R\text{CoO}_3$  shows a unique electronic phase change with change of temperature.<sup>5</sup> The ground state of  $\text{LaCoO}_3$  is a nonmagnetic insulator:  $\text{Co}^{3+}$  shows nominally the  $3d^6$  configuration and forms the singlet ( $S=0; t_{2g}^6$ ) state due to the crystal field splitting ( $10Dq$ ) barely dominating over the Hund's-rule coupling.  $\text{LaCoO}_3$  undergoes the spin state transition around 100 K from the low-spin ( $S=0$ ) to the high-spin ( $S=2$ ) or more likely to the intermediate-spin ( $S=1$ ) state,<sup>6-13</sup> while keeping an electrically insulating nature. With further increase of temperature, electrical conduction of  $\text{LaCoO}_3$  shows a crossover behavior around 500 K from a thermally activated semiconductive to a conducting state with metallic resistivity ( $\approx 1 \times 10^{-3} \Omega \text{ cm}$ ) (Ref. 14) and metallic Hall coefficient ( $\approx 1 \times 10^{-4} \text{ cm}^3/\text{C}$ ).<sup>15</sup> The important aspect of such successive electronic phase changes is that the magnitude of the charge gap ( $\geq 0.1$  eV) (Ref. 14) differs significantly from that of the spin gap (0.02–0.03 eV) and also from the energy scale of IM transition temperature ( $k_B T_{\text{IM}} \approx 0.05$  eV). This is contrasted by the case of the *nonmagnetic*  $3d$  compound

$\text{FeSi}$ ,<sup>16,17</sup> in which both gap energies are nearly identical ( $\approx 700$  K). As in the aforementioned case of  $\text{RNiO}_3$ , an explicit consideration of electron correlation would be necessary for understanding the IM phenomena in  $\text{LaCoO}_3$  and other related  $R\text{CoO}_3$ . In this view, a systematic control of the  $p$ - $d$  mixing (or the one-electron bandwidth  $W$ ) will be useful for the investigation of the IM transition and this can be best achieved by the systematic replacement of the  $R$ -site as in other  $R\text{MO}_3$  perovskites.<sup>4,18,19</sup> In the case of  $R\text{CoO}_3$  ( $R=\text{La, Pr, Nd, Sm, Eu, and Gd}$ ), we may change the Co-O-Co bond angle ( $\theta$ ) from  $\approx 164^\circ$  ( $R=\text{La}$ ) (Ref. 5) to around  $150^\circ$  ( $R=\text{Gd}$ ).<sup>20</sup> This may correspond to a change in  $t_{pd}$  by  $\approx 10\%$ , provided that  $t_{pd}$  nearly scales with  $\cos\theta$ . Here we show systematic variation of  $T_{\text{IM}}$  as well as transport and optical charge gaps for  $R\text{CoO}_3$  and argue the nature of the IM transition.

Crystals of  $R\text{CoO}_3$  ( $R=\text{La, Pr, Nd, Sm, Eu, and Gd}$ ) were grown by the floating-zone method. Starting materials were  $R_2\text{O}_3$  ( $R=\text{La, Nd, Sm, Eu, Gd}$ ),  $\text{Pr}_6\text{O}_{11}$ , and  $\text{CoO}$ . The raw materials were weighed to a prescribed ratio, mixed, and ground in a ball mill. The mixtures were heated in air at  $1050^\circ\text{C}$  for 12 h. Then, prereacted mixtures were reground and pressed into cylindrical form of feed rods (typically 5 mm  $\phi \times 60$  mm). The crystals were grown with use of a floating zone furnace equipped with two halogen incandescent lamps and double hemielliptical focusing mirror. The feed and seed rods were rotated in opposite directions at a relative speed of 40 rpm and the melted zone was vertically scanned at a speed of 1.5 mm/h in 5 atm oxygen atmosphere. Powder diffraction x-ray patterns showed that the sample of  $\text{LaCoO}_3$  was a slightly distorted perovskite with rhombohedral structure ( $R\bar{3}c$ ) and all the other samples ( $R=\text{Pr, Nd, Sm, Eu, Gd}$ ) were orthorhombically distorted ( $Pbnm$ ) at room temperature, which are in accord with the literature.<sup>5,21,22</sup>

In Fig. 1, we show the temperature dependence of electrical resistivity for crystals of  $R\text{CoO}_3$  ( $R=\text{La, Pr, Nd, Sm, Eu, and Gd}$ ). The substitution of the  $R$  site with smaller ions (from La toward Sm) increases resistivity over a whole temperature region. All the compounds show a gradual but significant decrease (down to a metallic value of  $10^{-3} \Omega \text{ cm}$ ) in resistivity at temperatures of 400–600 K. The transitional region shifts to higher temperature with a decrease of ionic

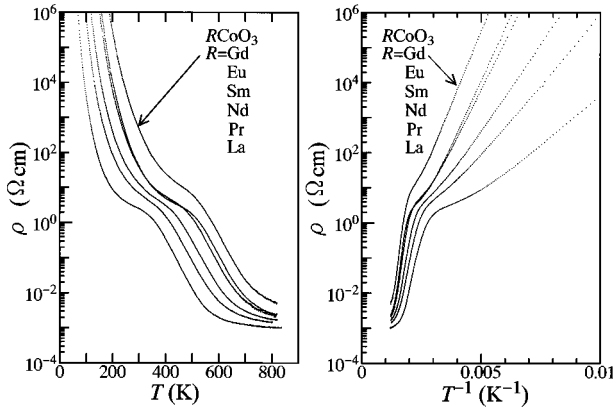


FIG. 1. Dependence of electrical resistivity ( $\rho$ ) on (a) temperature ( $T$ ) and (b) inverse of temperature ( $T^{-1}$ ) for crystals of  $R\text{CoO}_3$  ( $R = \text{La, Pr, Nd, Sm, Eu, and Gd}$ ).

radius of  $R$ . Such a systematic change of resistivity with  $R$  ensures the quality of these crystals and implies a systematic change of the charge gap. The low-temperature high-resistive state shows a thermal activation type conduction as clearly seen in the right panel of Fig. 1. (In the high-temperature region,  $T^{-1} < 0.02 \text{ K}^{-1}$ , the plot seemingly shows a large activation energy. However, this is ascribed to a rapid closing of the gap with an increase of temperature above 300 K, which gives rise to a gradual insulator-metal transition.) With a decrease of the  $R$ -site ionic radius or equivalently with a decrease of the  $p$ - $d$  hybridization, the activation energy increases systematically from 0.10 eV for  $R = \text{La}$  to 0.34 eV for  $R = \text{Gd}$ .

To argue the insulator-metal behavior in more detail over a wide temperature region, we show in Fig. 2 the temperature dependence of the quantity  $d \ln_{10} \rho / d(T^{-1})$ , which would represent the activation energy ( $\Delta_a$ ) in the case of thermally activated conduction. Large peaks, which signal the steep insulator-metal crossover, significantly shift to higher temperature with a decrease of  $R$ -site ionic radius (La

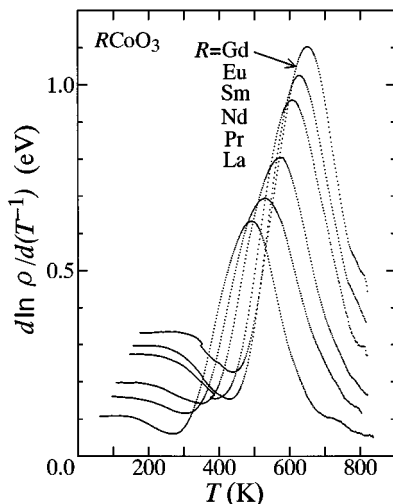


FIG. 2. The quantity  $d \ln \rho / d(T^{-1})$  plotted against temperature ( $T$ ) for a series of  $R\text{CoO}_3$  ( $R = \text{La, Pr, Nd, Sm, Eu, and Gd}$ ). The ordinate, if constant, would represent the thermal activation energy.

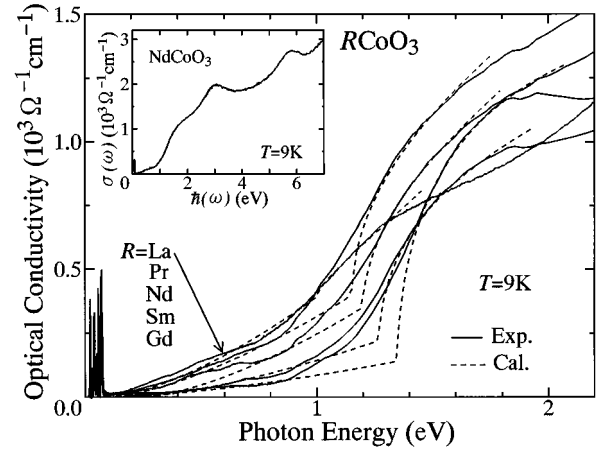


FIG. 3. Optical conductivity  $\sigma(\omega)$  spectra for  $R\text{CoO}_3$  at 9 K. Inset exemplifies the overall feature for  $\text{NdCoO}_3$ . Spiky peaks below 0.1 eV are due to optical phonons. Dashed lines are the best-fit results with the model function for the indirect-gap plus direct-gap transitions (see text).

$\rightarrow \text{Sm}$ ). Plateaus of  $d \ln_{10} \rho / d(T^{-1})$  observed at low temperatures (e.g., 60–150 K for  $\text{LaCoO}_3$ ) correspond to the thermally activated conduction with well-defined  $\Delta_a$ ; the  $\Delta_a$  value shows a systematic change with the replacement of  $R$ . The decrease of the  $R$ -site ionic radius gives rise to an increase in the lattice distortion and a decrease in the Co-O-Co bond angle. Variation of the charge gap, which should depend on the transfer integral of antibonding orbitals between  $\text{O}2p(\sigma)$  and  $\text{Co}3d(e_g)$  and hence should be crucially affected by such an  $R$ -site replacement, is likely to be an origin of variation of  $\Delta_a$ . This is also evidenced by optical spectroscopy (*vide infra*). It is worth noting here that a typical gap energy as given by  $2\Delta_a$  (for example,  $\sim 2300 \text{ K}$  for  $\text{LaCoO}_3$  and  $8000 \text{ K}$  for  $\text{GdCoO}_3$ ) is by far larger than  $T_{\text{IM}}$  ( $\sim 480 \text{ K}$  for  $\text{LaCoO}_3$  and  $650 \text{ K}$  for  $\text{GdCoO}_3$ ). Such a large discrepancy implies that the insulator-metal crossover in  $R\text{CoO}_3$  cannot be simply argued in terms of a narrow-gap semiconductor. The spin-gap for a thermal excitation to high-spin ( $t_{2g}^4 e_g^2$ ) or intermediate-spin ( $t_{2g}^5 e_g^1$ ) (Ref 13) state is known to be quite small [ $\approx 300 \text{ K}$  (Ref. 14) or  $\approx 230 \text{ K}$  (Ref. 23)] in  $\text{LaCoO}_3$ . Such a small spin-gap implies that  $\sim 85\%$  (80%) of Co ions are already excited to the high-spin (or intermediate-spin) state at room temperature.<sup>23</sup> Thus we cannot relate the change in transport property with the spin state transition.

We show in Fig. 3 optical conductivity spectra for  $R\text{CoO}_3$  at 9 K, which were derived by the Kramers-Kronig (KK) analysis of the reflectivity spectra. Measurements of reflectivity spectra were done for the photon energy region between 0.01 eV and 35 eV on specularly polished surfaces of the samples using Fourier spectroscopy (0.01–0.8 eV) and grating spectroscopy (0.6–35 eV). The reflectivity data above 6 eV, which were necessary to execute the accurate Kramers-Kronig transformation, were obtained using a synchrotron radiation at INSSOR, Institute for Solid State Physics, University of Tokyo, as a light source. The 9 K spectra can be viewed as representing the electronically ground state. The inset shows the spectrum for  $\text{NdCoO}_3$  in a

larger energy scale as a representative for the whole feature of spectra. The spectrum consists of three peaks at  $\sim 1.3$  eV, 3.0 eV, and 5.8 eV. According to the calculation based on the local density approximation (LDA+ $U_2$  model<sup>3</sup>), these bands correspond to the charge transfer excitations to the Co  $e_g$  band from the bonding and antibonding states consisting of Co  $t_{2g}$  and O  $2p$  states. In the ground state configuration, the lowest excitation may bear a character of the charge-transfer transition between the filled O  $2p$  states and the empty  $e_g$  states.<sup>2</sup>

In the low-energy spectra for  $R\text{CoO}_3$  below 2 eV (Fig. 3), the conductivity shows a gradual onset at 1–1.5 eV, while a residual broad tail is present at 0.1–1 eV. (Spiky structures below 0.1 eV are due to the optical phonon modes.) With the  $R$  replacement from La to Gd, the spectral onset shifts to higher energy. Sarma *et al.*<sup>24</sup> have pointed out by the LDA band calculation that the band gap in  $\text{LaCoO}_3$  is an indirect type, which is consistent with the broad spectral feature in the gap region as observed for  $\text{LaCoO}_3$ . A similar view of the indirect gap is likely to hold for a series of  $R\text{CoO}_3$  crystals. To estimate a change in the band gap, we fitted the spectra with the following model function:

$$\sigma(\omega) = A(\hbar\omega - E_{g,i})^{3/2} + B(\hbar\omega - E_{g,d})^{1/2}, \quad (1)$$

where  $E_{g,i}$  and  $E_{g,d}$  are gap energies for the indirect and the direct transitions, respectively, and  $A, B$  are the respective spectral weight. Dashed lines in Fig. 3 indicate the best-fit results for the respective spectra which clearly indicate the increase in the direct gap. The indirect gap  $E_{g,i}$  is difficult to determine accurately due to a blurred feature of the conductivity onset. We have tentatively set  $E_{g,i} = 0.10$  eV in common for all  $R\text{CoO}_3$  and evaluated the direct gap  $E_{g,d}$  for further quantitative analysis. (It was confirmed that the obtained  $E_{g,d}$  value is insensitive to a choice of the  $E_{g,i}$  value.) Because of the too simplified model function Eq. (1), the determined  $E_{g,d}$  value has still ambiguity in its absolute magnitude. Nevertheless, a systematic shift of  $E_{g,d}$  with  $R$  is quite clear in Fig. 3 and hence relative change in  $E_{g,d}$  values can bear a quantitative meaning for the measure of the charge-gap variation in  $R\text{CoO}_3$ .

We show in Fig. 4 observed energy gaps and IM transition temperatures against the tolerance factor,  $(\tilde{t} \equiv (r_R + r_O) / \sqrt{2}(r_{\text{Co}} + r_O))$ ,<sup>25,26</sup> which is relating to distortion of the perovskite lattice and hence the degree of the  $p$ - $d$  hybridization. Solid circles represent the optical gap  $E_{g,d}$  for the direct transition obtained by the fitting procedure shown in Fig. 3, while solid squares and open circles represent the transport gap ( $2\Delta_a$ ) and  $k_B T_{\text{IM}}$  (and also  $10 k_B T_{\text{IM}}$

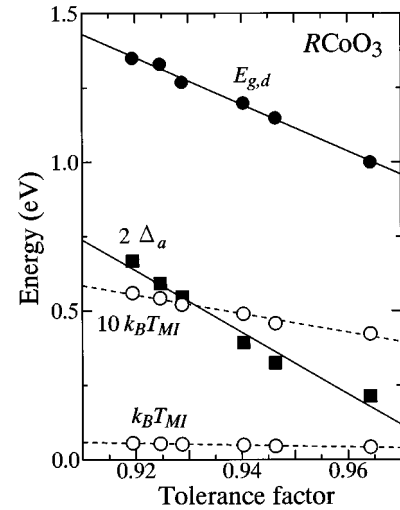


FIG. 4. Characteristic energies against the tolerance factor for a series of  $R\text{CoO}_3$ . Solid circles and solid squares represent the gap energies for the optical (direct) transition ( $E_{g,d}$ ) and for the charge transport ( $2\Delta_a$ ;  $\Delta_a$  being the activation energy), respectively, in the low-temperature insulating state. Open circles indicate temperatures ( $k_B T_{\text{IM}}$ ) of the insulator-metal transition as well as their magnification ( $10k_B T_{\text{IM}}$ ) for a better comparison.

for reference) as derived from Fig. 2. An energy value of  $k_B T_{\text{IM}}$  is by far smaller than  $2\Delta_a$  for all the  $R\text{CoO}_3$  crystal, as mentioned above, and the variation of  $k_B T_{\text{IM}}$  with  $R$  is not so significant as  $2\Delta_a$  or  $E_{g,d}$ . The  $E_{g,d}$  and  $2\Delta_a$  shows a nearly parallel behavior as a function of  $\tilde{t}$ . According to the empirical relation between the metal-oxygen-metal bond angle ( $\theta$ ) and  $\tilde{t}$  in distorted perovskites,<sup>27,28</sup>  $\theta$  in  $R\text{CoO}_3$  may change nearly linearly with  $\tilde{t}$  from  $\approx 164^\circ$  for  $\text{LaCoO}_3$  (Ref. 5) down to around  $150^\circ$  for  $\text{GdCoO}_3$ .<sup>20</sup> The  $p$ - $d$  transfer interaction  $t_{pd}$  approximately scales with  $\cos\theta$ , indicating that  $t_{pd}$  changes also nearly linearly with  $\tilde{t}$  by  $\approx 10\%$  between  $R = \text{La}$  and  $\text{Gd}$  in  $R\text{CoO}_3$ . The observed change of the gap magnitude is quite large as compared with the change in  $t_{pd}$ . Such a critical change in the charge gap with  $t_{pd}$  as well as an anomalously low  $T_{\text{IM}}$  as compared with the gap magnitude suggests an important role of electron correlation for the origin of the charge-gap formation below  $T_{\text{IM}}$ . Thus, the IM transition in  $R\text{CoO}_3$  may bear a character of the Mott transition rather than that of the narrow-gap semiconductor.<sup>28</sup>

We are grateful to N. Hamada and H. Takagi for enlightening discussions. This work was supported in part by a Grant-In-Aid for Scientific Research from the Ministry of Education, Science and Culture, Japan, and by NEDO.

<sup>1</sup>C. N. R. Rao and G. V. S. Rao, Phys. Status Solidi A **1**, 597 (1970).

<sup>2</sup>T. Arima, Y. Tokura, and J. B. Torrance, Phys. Rev. B **48**, 17006 (1993).

<sup>3</sup>I. Solovyev, N. Hamada, and K. Terakura, Phys. Rev. B **53**, 7158 (1996).

<sup>4</sup>J. B. Torrance, P. Lacorre, A. I. Nazzari, E. J. Ansaldo, and Ch.

Niedermayer, Phys. Rev. B **45**, 8209 (1992).

<sup>5</sup>G. Thornton, B. C. Tofield, and A. W. Hewat, J. Solid State Chem. **61**, 301 (1986).

<sup>6</sup>J. B. Goodenough, J. Chem. Phys. Solids **6**, 287 (1958).

<sup>7</sup>C. S. Naiman, R. Gilmore, B. DiBartolo, A. Linz, and R. Santoro, J. Appl. Phys. **36**, 1044 (1965).

<sup>8</sup>V. G. Bhide, D. S. Rajoria, G. R. Rao, and C. N. R. Rao, Phys.

- Rev. B **6**, 1021 (1972).
- <sup>9</sup>K. Asai, P. Gehring, H. Chou, and G. Shirane, Phys. Rev. B **40**, 10982 (1989).
- <sup>10</sup>L. Richter, S. D. Bader, and M. B. Brodsky, Phys. Rev. B **22**, 3059 (1980).
- <sup>11</sup>S. R. Barman and D. D. Sarma, Phys. Rev. B **49**, 13979 (1994).
- <sup>12</sup>M. Itoh, M. Sugahara, I. Natori, and K. Motoya, J. Phys. Soc. Jpn. **64**, 3967 (1995).
- <sup>13</sup>M. A. Korotin, S. Y. Ezhov, I. V. Solovyev, V. I. Anisimov, D. I. Khomskii, and G. A. Sawatzky, Phys. Rev. B (to be published).
- <sup>14</sup>S. Yamaguchi, Y. Okimoto, H. Taniguchi, and Y. Tokura, Phys. Rev. B **53**, R2926 (1996).
- <sup>15</sup>H. Takagi *et al.* (unpublished).
- <sup>16</sup>Z. Schlesinger *et al.*, Phys. Rev. Lett. **71**, 1748 (1993).
- <sup>17</sup>P. Nyhus, S. L. Cooper, and Z. Fisk, Phys. Rev. B **51**, 15626 (1995).
- <sup>18</sup>Y. Okimoto, T. Katsufuji, Y. Okada, T. Arima, and Y. Tokura, Phys. Rev. B **51**, 9581 (1995).
- <sup>19</sup>H. Y. Hwang, S-W. Cheong, P. G. Radaelli, M. Marezio, and B. Batlogg, Phys. Rev. Lett. **75**, 914 (1995).
- <sup>20</sup>To the best of our knowledge, the detailed structure analysis has not been done for  $R\text{CoO}_3$  apart from  $R=\text{La}$  (Ref. 5). According to the systematic behavior of the  $\text{GdFeO}_3$ -type structure with variation of the tolerance factor (Refs. 27 and 28), we could approximately estimate a change in the Co-O-Co bond angle  $\theta$ .
- <sup>21</sup>A. Kappatsch, S. Quezel-Ambrunaz, and J. Sivardière, J. Phys. France **31**, 369 (1970).
- <sup>22</sup>P. M. Raccach and J. B. Goodenough, Phys. Rev. **155**, 932 (1967).
- <sup>23</sup>If the excited spin-state is the intermediate-spin state, the molecular field approximation (Ref. 14) gives a smaller value of the spin-gap ( $\Delta=230$  K). The density of excited intermediate-spin (or high-spin) states calculated by this model is as high as 80% (or 85%) per Co site at 300 K.
- <sup>24</sup>D. D. Sarma, N. Shanthi, S. R. Barman, N. Hamada, H. Sawada, and K. Terakura, Phys. Rev. Lett. **75**, 1126 (1995).
- <sup>25</sup>P. Poix, C. R. Acad. Sci. (Paris) **270C**, 1852 (1970).
- <sup>26</sup>P. Poix, C. R. Acad. Sci. (Paris) **268C**, 1139 (1969).
- <sup>27</sup>M. Marezio, J. P. Remeika, and P. D. Dernier, Acta Crystallogr. Sect. B **26**, 2008 (1970).
- <sup>28</sup>D. A. MacLean, Hok-Nam Ng, and J. E. Greedan, J. Solid State Chem. **30**, 35 (1979).